

# Parametric deconvolution of positive spike trains

Technical Report No. 585

Lei Li\*  
Florida State University

Terence P. Speed†  
University of California, Berkeley

May 6, 2000

## Abstract

This paper describes a parametric deconvolution method (PDPS) appropriate for a particular class of signals which we call spike-convolution models. These models arise when a sparse spike train—Dirac deltas according to our mathematical treatment—is convolved with a fixed point-spread function, and additive noise or measurement error is superimposed. We view deconvolution as an estimation problem, regarding the locations and heights of the underlying spikes, as well as the baseline and the measurement error variance as unknown parameters. Our estimation scheme consists of two parts: model fitting and model selection. To fit a spike-convolution model of a specific order, we estimate peak locations by trigonometric moments, and heights and the baseline by least squares. The model selection procedure has two stages. Its first stage is so designed that we expect a model of a somewhat larger order than the truth to be selected. In the second stage, the final model is obtained using backwards deletion. This results in not only an estimate of the model order, but also an estimate of peak locations and heights with much smaller bias and variation than that found in a direct trigonometric moment estimate. A more efficient maximum likelihood estimate can be calculated from these estimates using a Gauss-Newton algorithm. We also present some relevant results concerning the spectral structure of Toeplitz matrices which play a key role in the estimation. Finally, we illustrate the behavior of these estimates using simulated and real DNA sequencing data.

**Abbreviated title: Parametric deconvolution**

**AMS 1991 subject classification: Primary 62F10; Secondary 62F12, 86A22.**

**Key words and phrases: deconvolution, spike train, model selection, DNA sequencing, Toeplitz matrix.**

---

\*Supported by NSF grant DMS-9971698

†Supported by DOE grant DE-FG03-97ER62387

# 1 Introduction and background

Deconvolution is used in many scientific disciplines, including geophysics, spectroscopy, chromatography and pharmacokinetics. In abstract form, an unobserved signal  $x(t)$  is blurred by a known point spread function  $w$ , resulting in an observed signal  $y(t)$ . Mathematically, this can be represented in terms of the convolution operation  $*$ :  $y = w * x$ . The task of deconvolution is to reconstruct the unobserved signal  $x$  from the observed signal  $y$ . The point spread function is assumed to be known throughout this paper. An additive measurement error is also assumed in  $y$  in all discrete situations discussed.

Our motivation is the problem of base-calling in DNA sequencing. The Sanger sequencing technique is a combination of enzymatic reactions, electrophoresis and fluorescence-based detection, see [1]. This procedure produces a four-component vector time series. Base-calling is the analysis part of DNA sequencing, which attempts to recover the underlying DNA sequence from the vector time series. Figure 1 shows a segment of one channel of such a series (This series is different from the original sequencing data because of the “cross talk” phenomenon. We here pass over this issue, and refer to [21] for details). Typically, each major peak in the series corresponds to one base. As sequencing progresses, electrophoretic diffusion spreads peaks more and more. In regions where there are multiple occurrences of the same base, several successive peaks may merge into one large block. In this situation, base-calling is far more difficult. A number of studies exist of the errors made by one widely-used base-calling system, see [3, 17, 18]. These reports show that errors associated with runs of the same base constitute more than half of the total errors. Furthermore, this kind of error causes more serious difficulties in later analysis than other kinds. For this reason, it seems important to try and do better in resolving peaks, and this is the motivation of the research we report here.

The literature on deconvolution is rich and scattered across a wide variety of fields. Frequently, deconvolution is an ill-posed inverse problem, see Jansson [13]. Two techniques, regularization and exploiting bound or non-negativity constraints on the unknown functions, have been proved to be useful in dealing with ill-posedness. Regularization was introduced by Tikhonov [30], and has been well studied since then. For example, the long-standing iterative deconvolution method of Van Cittert, see Jansson [13], can be viewed as a regularization method. Jansson [13] adjusted this regularization method, adds non-negativity constraints to the unknown function, and applies it successfully to problems in spectroscopy.

Maximum entropy deconvolution can also be regarded as a regularization procedure, one which only applies to nonnegative signals, see [10, 11]. Donoho et al. [5] showed this procedure has certain advantages such as signal-to-noise enhancement and super-resolution when the signal is nearly-black. Stark and Parker [29] proposed some new algorithms to solve this type of constrained minimization problems.

The deblurring method introduced by Shepp and Vardi [27], and Vardi and Lee [32] uses maximum likelihood estimation under a Poisson or a multinomial model. Again it is assumed that the unknown function is nonnegative. Snyder et al. [28] obtained a similar algorithm as a solution to a general Fredholm integral equation of the first kind. They derive the formula by minimizing Csiszár’s I-divergence, which is closely related to the concept of likelihood. Richardson [26], Kennett et al. [14, 15, 16], and Di Gesù et al. [4] obtained the same result from a more intuitive Bayesian point of view, and term it as “Bayesian deconvolution”. All of these methods could be

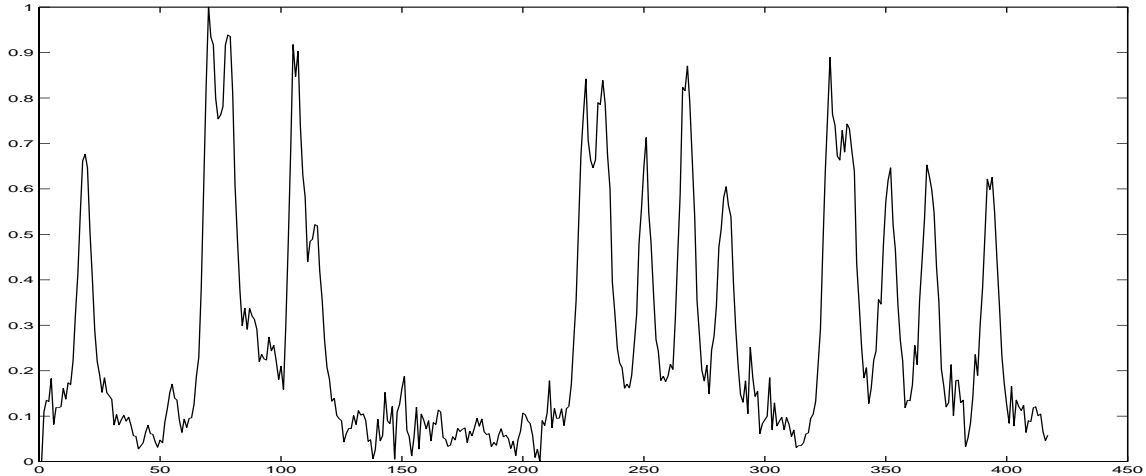


Figure 1: A segment slab gel electrophoresis sequencing data (provided by the engineering group at Lawrence Berkeley National Laboratory).

used in the base-calling problem, and their behavior on DNA sequencing data can be found in [20].

Poskitt et al [25] described a double-blind deconvolution method to analyze post-synaptic currents in nerve cells. This analysis is based on an elegant statistical model, and the estimator is derived by minimizing the quasi-profile-likelihood. Though the data from post-synaptic currents in nerve cells are different from DNA sequencing data, we find the likelihood structures of the two models proposed for each problem have some similarities. Therefore, we can borrow some ideas from [25] to study the deconvolution problem in DNA sequencing.

Motivated by the DNA sequencing data, we define what we call the spike-convolution model, in which the unknown function is represented as a linear combination of a finite number of positive spikes (Dirac functions) together with a constant baseline. In this model, deconvolution is nothing but a standard parameter estimation problem, where the parameters include the number, locations and heights of the underlying spikes, the baseline and the measurement error variance. Our estimation procedure uses the spectral properties of Toeplitz matrices, least squares, and statistical model selection techniques, and we call it parametric deconvolution of positive spikes (PDPS).

The paper is arranged as follows. In Section 2 we introduce the spike-convolution model and some notation, discuss several aspects such as identifiability, and outline the estimation procedure. In Section 3 we study spectral structures of Toeplitz matrices constructed from trigonometric moments, and present algorithms and asymptotics of the trigonometric moments estimates. In Section 4 we describe the algorithms and asymptotics of the maximum likelihood estimates. In Section 5 we propose our ultimate method, which is a package including a model fitting procedure and a two-stage model selection procedure. Section 6 contains a simulation study of the proposed methodologies. Finally, we apply PDPS to real DNA sequencing data, and compare the result with that using another nonparametric deconvolution method. Several other practical issues of PDPS are also discussed. The appendix contains the proofs and the relevant mathematical details.

## 2 The spike-convolution model

Throughout the paper, the point spread function  $w(\cdot)$  is assumed to be known, and to satisfy the following conditions, where  $v_k = \frac{1}{2\pi} \int_{-\pi}^{\pi} w(t) e^{ikt} dt$  are  $w$ 's Fourier coefficients.

1. It has finite support  $(-\kappa_1, \kappa_2)$ , where  $0 < \kappa_1, \kappa_2 < \pi$ ;
2.  $w(\cdot) \in C^2[-\pi, \pi]$ ;
3.  $v_k \neq 0$ , for  $k = 0, \pm 1, \dots, \pm K_0$ .

The last assumption is described by people as requiring that there is no hole in the Fourier transform of the point spread function. It worth mentioning that  $w(\cdot)$  is not necessarily nonnegative or causal. There exist studies of the shape of the point spread function in DNA sequencing, see [23] for references, and the determination of the width of the point spread function is another matter worthy of attention. However, these issues are not critical to the present work, and so we pass over them here. The signal to be estimated is assumed to have the following form,

$$x(t) = A_0 + \sum_{j=1}^p A_j \delta(t - \tau_j), \quad (1)$$

where  $\delta(\cdot)$  is the Dirac delta function. We assume the coefficients  $A_j$  of the Dirac functions are positive, and refer to them as ‘‘heights’’ of the spikes. Thus the underlying signal  $x(t)$  is a linear combination of a finite number of spikes with positive heights, together with a constant baseline. We also assume  $-\pi + \kappa_1 < \tau_1 < \dots < \tau_p < \pi - \kappa_2$ . Hence the support of the convolution  $y$  of  $w$  and  $x$  will stay in the range  $[-\pi, \pi]$ . Explicitly, we have

$$y(t) = A_0 + \sum_{j=1}^p A_j w(t - \tau_j) = (x * w)(t), \quad t \in [-\pi, \pi], \quad (2)$$

where the time range has been scaled to  $[-\pi, \pi]$  for convenience. We have assumed there are no peaks near the two ends. In real DNA sequencing, we can always cut the raw data into pieces at valley points, and apply the deconvolution to each piece separately. The observations  $\{z(t_l)\}$  are a sample of the above model, corrupted by measurement errors which are assumed to be additive:

$$z(t_l) = y(t_l) + \epsilon(t_l) = A_0 + \sum_{j=1}^p A_j w(t_l - \tau_j) + \epsilon(t_l), \quad (3)$$

where  $t_l = \frac{2\pi l}{n}$ ,  $l = -[\frac{n}{2}], \dots, 0, \dots, [\frac{n}{2}] - 1$  if  $n$  is even, or  $l = -[\frac{n}{2}], \dots, 0, \dots, [\frac{n}{2}]$  if  $n$  is odd. The  $\{\epsilon(t_l)\}$  are supposed to be i.i.d. with  $E(\epsilon(t_l)) = 0$ ,  $Var(\epsilon(t_l)) = \sigma^2$ , and a finite third moment.

Before we proceed, we introduce some notation. We denote the signal in the spike-convolution model (2) by  $SC(w; p; \mathbf{A}; \boldsymbol{\tau})$  where  $\mathbf{A}$  and  $\boldsymbol{\tau}$  respectively represent  $\{A_j\}$  and  $\{\tau_j\}$ , and formally denote the signal  $x$  in (1) by  $SC(\delta; p; \mathbf{A}; \boldsymbol{\tau})$ . We define the inner product of two functions  $y_1(t)$  and  $y_2(t)$ , belonging to  $L^2[-\pi, \pi]$ , by  $\langle y_1, y_2 \rangle = \frac{1}{2\pi} \int_{-\pi}^{\pi} y_1(t) y_2(t) dt$ . For functions  $z_1(t)$  and  $z_2(t)$  well defined at the lattice points  $t_l = \frac{2\pi l}{n}$ , we also define the following inner product

$$\langle z_1, z_2 \rangle_n = \begin{cases} \frac{1}{n} \sum_{l=-[\frac{n}{2}]}^{[\frac{n}{2}]} z_1(t_l) z_2(t_l), & \text{if } n \text{ is odd} \\ \frac{1}{n} \sum_{l=-[\frac{n}{2}]}^{[\frac{n}{2}]-1} z_1(t_l) z_2(t_l), & \text{if } n \text{ is even} \end{cases}.$$

The norms induced by  $\langle \cdot, \cdot \rangle$  and  $\langle \cdot, \cdot \rangle_n$  are denoted by  $\| \cdot \|$  and  $\| \cdot \|_n$  respectively.

The Hilbert-Schmidt theory for Fredholm integral equations of the first kind assumes that the signal  $x(t)$  is in  $L^2[\pi, \pi]$ , and thus excludes the Dirac functions. Consequently, the signal reconstructed by methods within that framework will not contain any Dirac functions. This means that only incomplete deconvolution would be achieved if (2) were the truth. We prefer to regard deconvolution as a problem of parameter estimation, and this can result in a complete deconvolution.

The parameters in a  $SC(w; p; \mathbf{A}; \boldsymbol{\tau})$  model include the number, locations and heights of the peaks, and the baseline. Although these parameters are closely related, they play quite different roles from the perspective of statistical estimation, and it seems very difficult to estimate them all, simultaneously and efficiently, in one step. The difficulty lies in the irregular structure of the parameter space. For example, suppose we have a spike-convolution model with three positive peaks. If we let the height of one peak tend to zero, then the limiting model can only be regarded as a spike-convolution model with two peaks, for we require peak heights to be positive. Following this limiting process, the dimension of the parameter space changes. However, we have the following result saying that a spike-convolution model of order  $p$  cannot arbitrarily well be approximated by models of smaller orders.

**Theorem 2.1** *Let  $y(t)$  be a  $SC(w; p; \mathbf{A}; \boldsymbol{\tau})$  model. Then we have:  $\inf_{\bar{y}} \| y - \bar{y} \| = d > 0$ , where the infimum is taken over all  $\bar{y} \in SC(w; l; \bar{\mathbf{A}}; \bar{\boldsymbol{\tau}})$ ,  $l < p$ .*

A relating problem in signal processing is to estimate the so-called hidden frequencies  $\omega_j$  in the following model

$$s_t = \sum_{j=1}^p A_j \cos(t\omega_j + \theta_j) + \epsilon_t, \quad (4)$$

where the  $A_j$  are positive and  $\epsilon_t$  is white noise. In fact, the spectral density function of the above process, in the generalized sense, is a constant plus jumps occurring at the  $\omega_j$ , with corresponding heights  $A_j$ . This is exactly the signal to be reconstructed in Model (2). Apart from the point spread function, the two problems are Fourier duals of each other. In order to estimate the hidden frequencies, Pisarenko [24] suggested a method using the Toeplitz matrices constructed from autocovariance functions. We exploit a similar idea as part of our estimation procedure.

Our estimation procedure consists of several steps. In Algorithm 3.1, we estimate the peak locations by connecting deconvolution with the spectral structure of Toeplitz matrices constructed from the Fourier coefficients of the observations. The peak heights of the estimated locations can be estimated either by a trigonometric moment method—Algorithm 3.2, or by least squares, where the latter exploits the connection between spike-convolution models and hypothetical linear regressions, see Algorithm 5.1. This leaves us with the task of estimating the number of peaks, one usually regarded as a model selection problem. In our method, models of each candidate order have to be fitted before model selection takes place. The model selection strategy described in Algorithm 5.2 consists of two stages. First we choose a model which should come close to including the true model as a submodel, as overfitting is not completely suppressed at this step. We then use a modified GIC criterion together with a backward deletion procedure to obtain our final model. The resulting estimate can further be tuned by an optional step: maximizing likelihood if the distribution of the measurement errors is assumed known, see Section 4. Under the assumption of normal errors, we calculate the Fisher information matrix of the spike-convolution model, whose inverse gives the nominal standard errors of estimates. Note that these standard errors will not

have taken into account the model selection process. The computation of the maximum likelihood estimate or one-step estimate can be carried out by Gauss-Newton algorithm. Please keep in mind that Section 3 and 4 are about inference given the model order  $m$ —the number of spikes included in the spike-convolution model. This is a brief description of PDPS, which will be explained more fully in the rest of the paper.

### 3 The trigonometric moment estimates

Throughout this section, we assume the model order  $m$  is given. The connection between the trigonometric moments and the parameters in a spike-convolution model can be given using the spectral structure of Toeplitz matrices as follows.

**Theorem 3.1** *Let the Fourier coefficients of  $y(t)$ , which follows  $SC(w; m; \mathbf{A}; \boldsymbol{\tau})$  with  $m \leq K_0$ , be  $f_k = \langle y(t), e^{ikt} \rangle$ , for  $k = 0, \pm 1, \dots$ . First, write  $g_0 = f_0$  and  $g_k = f_k v_0 / v_k$ , for  $0 < k \leq K_0$ . Next, form the Toeplitz matrices  $G_m = (g_{j-i})_{i,j=0,\dots,m}$ . Finally, write  $U^{(m)}(z) = \prod_{j=1}^m (z - e^{i\tau_j}) = \sum_{j=0}^m \alpha_j z^j$ . Then we have*

1.

$$\begin{cases} f_0 &= A_0 + (\sum_{j=1}^m A_j) v_0 \\ f_k &= (\sum_{j=1}^m A_j e^{ik\tau_j}) v_k, \quad k \neq 0 \end{cases} \quad (5)$$

2.  $A_0$  is the smallest eigenvalue of  $G_m$  with multiplicity one and eigenvector  $(\alpha_0, \dots, \alpha_m)^T$ .

3. The  $\{A_j\}$  satisfy the following linear system:

$$v_0 \begin{pmatrix} 1 & 1 & \dots & 1 \\ e^{i\tau_1} & e^{i\tau_2} & \dots & e^{i\tau_m} \\ \vdots & \vdots & \ddots & \vdots \\ e^{i(m-1)\tau_1} & e^{i(m-1)\tau_2} & \dots & e^{i(m-1)\tau_m} \end{pmatrix} \begin{pmatrix} A_1 \\ A_2 \\ \vdots \\ A_m \end{pmatrix} = \begin{pmatrix} g_0 - A_0 \\ g_1 \\ \vdots \\ g_{m-1} \end{pmatrix}. \quad (6)$$

**Note:** When a Toeplitz matrix has distinct eigenvalues, the relation between eigenvalues and eigenvectors is one-to-one. For simplicity, we will use expressions such as “smallest eigenvector” to refer to the eigenvector corresponding to the smallest eigenvalue. The converse of the above theorem is also true in the following sense.

**Theorem 3.2** *Suppose we are given  $2m + 1$  complex numbers  $\{f_j, -m \leq j \leq m\}$ , where  $m \leq K_0$ ,  $\overline{f_j} = f_{-j}$ . Let  $g_0 = f_0$ , and  $g_k = f_k v_0 / v_k$ , for  $0 < k \leq K_0$ . Assume that the smallest eigenvalue  $A_0$  of the Toeplitz matrix  $G_m = (g_{j-i})_{i,j=0,\dots,m}$  has multiplicity 1. Let the smallest eigenvector be  $\alpha = (\alpha_0, \dots, \alpha_m)^T$ , and  $U^{(m)}(z) = \sum_{j=0}^m \alpha_j z^j$ . Then*

1.  $U^{(m)}(z)$  has  $m$  distinct roots exactly on the unit circle, which are denoted by  $\{e^{i\tau_j}\}$ .

2. Furthermore, if  $-\pi + \kappa_1 < \tau_1 < \dots < \tau_m < \pi - \kappa_2$ , then there exists a  $SC(w; m; \mathbf{A}; \boldsymbol{\tau})$  whose first  $m + 1$  Fourier coefficients are  $\{f_j, 0 \leq j \leq m\}$ . Its baseline and heights  $\{A_j\}$  are determined by the linear system (6), and the resulting heights are positive.

This result is of great significance for practical model fitting from the computational point of view, since the peak locations could be found by restricting the search of roots of  $U^{(m)}(z)$  to the unit circle. Starting from data  $z(t_l)$ , we estimate the trigonometric moments by  $\hat{f}_k = \langle z, e^{ikt} \rangle_n$ . Based on Theorem 3.2, for any given nonnegative integer  $m \leq K_0$ , we can input these empirical trigonometric moments into the following two algorithms.

**Algorithm 3.1 Trigonometric moment estimates of peak locations.**

1. *Deconvolution:* let  $\hat{g}_0 = \hat{f}_0$ ,  $\hat{g}_k = \hat{f}_k v_0/v_k$ , for  $k = \pm 1, \dots, \pm m$ .
2. *Computing the smallest eigenvalue-vector of the Toeplitz matrix:* construct the Toeplitz matrix  $\hat{G}_m = (\hat{g}_{j-i})$ , and compute its smallest eigenvalue  $\hat{A}_0^{(m)}$  (assuming its multiplicity is one), and corresponding eigenvector  $\hat{\alpha}^{(m)} = (\hat{\alpha}_0^{(m)}, \dots, \hat{\alpha}_m^{(m)})$ .
3. *Solving a polynomial:* on the unit circle, find the  $m$  distinct roots of  $\hat{U}^{(m)}(z) = \sum_{j=0}^m \hat{\alpha}_j^{(m)} z^j$ , which we denote by  $\{e^{i\hat{\tau}_j^{(m)}}\}$ ,  $j = 1, \dots, m$ .

**Algorithm 3.2 Trigonometric moment estimates of heights.**

*Solve the following Vandermonde linear system:*

$$v_0 \begin{pmatrix} 1 & 1 & \dots & 1 \\ e^{i\hat{\tau}_1^{(m)}} & e^{i\hat{\tau}_2^{(m)}} & \dots & e^{i\hat{\tau}_m^{(m)}} \\ \vdots & \vdots & \ddots & \vdots \\ e^{i(m-1)\hat{\tau}_1^{(m)}} & e^{i(m-1)\hat{\tau}_2^{(m)}} & \dots & e^{i(m-1)\hat{\tau}_m^{(m)}} \end{pmatrix} \begin{pmatrix} \hat{A}_1^{(m)} \\ \hat{A}_2^{(m)} \\ \vdots \\ \hat{A}_m^{(m)} \end{pmatrix} = \begin{pmatrix} \hat{g}_0 - \hat{A}_0^{(m)} \\ \hat{g}_1 \\ \vdots \\ \hat{g}_{m-1} \end{pmatrix}.$$

The output of these two algorithms is a  $SC(w; m; \hat{\mathbf{A}}^{(m)}; \hat{\boldsymbol{\tau}}^{(m)})$  whose first  $m+1$  Fourier coefficients are  $\hat{f}_k, k = 0, \dots, m$ . We make some remarks here. First, we have ignored the case when the multiplicity of  $A_0$  is greater than 1, since the Lebesgue measure of this singular case is zero. Second, strictly speaking, the fitted model makes sense only when  $-\pi + \kappa_1 < \hat{\tau}_1^{(m)} < \dots < \hat{\tau}_m^{(m)} < \pi - \kappa_2$ . We thus delete those peaks outside the legitimate range in the regression stage discussed later, and then estimate the heights of the remaining peaks by least squares, see Algorithm 5.1 for more details. Third, our numerical experiments carried out in MATLAB show these two algorithms are robust to round off and noise in the data. For example, the roots of  $\hat{U}^{(m)}(z)$  do indeed lie on the unit circle to the necessary accuracy. Finally, in the case that the observations are generated from a  $SC(w; p; \mathbf{A}; \boldsymbol{\tau})$ , if we take  $m = p$ , then  $\hat{\tau}_j$  and  $\hat{A}_j$  are the trigonometric moment estimates, which are consistent. Indeed, we have the following central limit theorem.

**Theorem 3.3**

$$\sqrt{n} [(\hat{A}_0, \hat{A}_1, \dots, \hat{A}_p, \hat{\tau}_1, \dots, \hat{\tau}_p)^T - (A_0, A_1, \dots, A_p, \tau_1, \dots, \tau_p)^T] \xrightarrow{d} N(0, V). \quad (7)$$

where  $V = 4 \pi^2 Q^{-1} P Q^{-T}$ ,

$$P = \frac{\sigma^2}{2} \text{diag}(2, |\frac{v_0}{v_1}|^2, \dots, |\frac{v_0}{v_p}|^2, |\frac{v_0}{v_1}|^2, \dots, |\frac{v_0}{v_p}|^2), \quad (8)$$

and

$$Q = \left( \begin{array}{c|cccc|cccc} 1 & 1 & 1 & \cdots & 1 & 0 & 0 & \cdots & 0 \\ 0 & \cos \tau_1 & \cos \tau_2 & \cdots & \cos \tau_p & -A_1 \sin \tau_1 & -A_2 \sin \tau_2 & \cdots & -A_p \sin \tau_p \\ \vdots & \vdots & \vdots & \ddots & \vdots & \vdots & \vdots & \ddots & \vdots \\ 0 & \cos p\tau_1 & \cos p\tau_2 & \cdots & \cos p\tau_p & -p A_1 \sin p\tau_1 & -p A_2 \sin p\tau_2 & \cdots & -p A_p \sin p\tau_p \\ \hline 0 & \sin \tau_1 & \sin \tau_2 & \cdots & \sin \tau_p & A_1 \cos \tau_1 & A_2 \cos \tau_2 & \cdots & A_p \cos \tau_p \\ \vdots & \vdots & \vdots & \ddots & \vdots & \vdots & \vdots & \ddots & \vdots \\ 0 & \sin p\tau_1 & \sin p\tau_2 & \cdots & \sin p\tau_p & p A_1 \cos p\tau_1 & p A_2 \cos p\tau_2 & \cdots & p A_p \cos p\tau_p \end{array} \right). \quad (9)$$

More algebra shows that the asymptotic variances of the  $\{A_j\}$  depends only on the  $\{\tau_j\}$ , while the asymptotic variances of the  $\{\tau_j\}$  depend not only on the configuration of the  $\{\tau_j\}$ , but also on the heights  $\{A_j\}$ . In fact, if we define  $A/\sigma$  to be the local signal-to-noise ratio, then the asymptotic standard deviation of  $\hat{\tau}_j$  is proportional to the reciprocal of its local signal-to-noise ratio.

## 4 The maximum likelihood estimates

Throughout this section, we assume the model order  $m$  is given. In general, trigonometric moment estimates are not as efficient as maximum likelihood estimates. However, starting from trigonometric moment estimates, which are  $\sqrt{n}$ -consistent, we can construct one-step estimates or find maximum likelihood estimates using Fisher scoring. In either case, we need to specify the error distribution to calculate the Fisher information matrix. Under the assumption of normal errors, the  $-2 \log \text{likelihood}$  of the observations generated from Model (3) is

$$n \log(2\pi\sigma^2) + \frac{1}{\sigma^2} \sum_l \left\{ z(t_l) - A_0 - \sum_{j=1}^p A_j w(t_l - \tau_j) \right\}^2. \quad (10)$$

More notation is needed in this section. We write  $\theta = (A_0, A_1, \dots, A_p, \tau_1, \dots, \tau_p)^T$ , and sometimes we use  $y_\theta(t)$  to denote  $SC(w; p; \mathbf{A}; \boldsymbol{\tau})$ . Denote the gradient vector by  $\nabla_\theta = (\partial \log L / \partial \theta)^T$ , and  $\nabla_{(\theta, \sigma^2)} = (\nabla_\theta^T, \partial \log L / \partial \sigma^2)^T$ . As usual, the Fisher information matrix is defined by  $I_{(\theta, \sigma^2)} = \frac{1}{n} E[\nabla_{(\theta, \sigma^2)} \nabla_{(\theta, \sigma^2)}^T]$ , and  $I_\theta = \frac{1}{n} E[\nabla_\theta \nabla_\theta^T]$ .

**Proposition 4.1** *Let  $\Psi_\theta = (\psi_{A_0}, \psi_{A_1}, \dots, \psi_{A_p}, \psi_{\tau_1}, \dots, \psi_{\tau_p})^T$ , where  $\psi_{A_0} = 1$ ,  $\psi_{A_j} = w(t - \tau_j)$ ,  $\psi_{\tau_j} = -A_j w'(t - \tau_j)$ ,  $j = 1, \dots, p$ . Then*

$$I_{(\theta, \sigma^2)} = \begin{pmatrix} I_\theta & \mathbf{0}_p^T \\ \mathbf{0}_p & \frac{1}{2\sigma^4} \end{pmatrix}, \quad (11)$$

where  $\mathbf{0}_p$  is a vector with  $p$  zeros, and

$$I_\theta = \frac{1}{\sigma^2} \langle \Psi_\theta, \Psi_\theta^T \rangle_n \longrightarrow \frac{1}{\sigma^2} \langle \Psi_\theta, \Psi_\theta^T \rangle. \quad (12)$$



Here  $\langle \Psi_\theta, \Psi_\theta^T \rangle$  is defined by

$$\left( \begin{array}{c|ccc|ccc} \langle \psi_{A_0}, \psi_{A_0} \rangle & \langle \psi_{A_0}, \psi_{A_1} \rangle & \cdots & \langle \psi_{A_0}, \psi_{A_p} \rangle & \langle \psi_{A_0}, \psi_{\tau_1} \rangle & \cdots & \langle \psi_{A_0}, \psi_{\tau_p} \rangle \\ \langle \psi_{A_1}, \psi_{A_0} \rangle & \langle \psi_{A_1}, \psi_{A_1} \rangle & \cdots & \langle \psi_{A_1}, \psi_{A_p} \rangle & \langle \psi_{A_1}, \psi_{\tau_1} \rangle & \cdots & \langle \psi_{A_1}, \psi_{\tau_p} \rangle \\ \vdots & \vdots & \ddots & \vdots & \vdots & \ddots & \vdots \\ \langle \psi_{A_p}, \psi_{A_0} \rangle & \langle \psi_{A_p}, \psi_{A_1} \rangle & \cdots & \langle \psi_{A_p}, \psi_{A_p} \rangle & \langle \psi_{A_p}, \psi_{\tau_1} \rangle & \cdots & \langle \psi_{A_p}, \psi_{\tau_p} \rangle \\ \hline \langle \psi_{\tau_1}, \psi_{A_0} \rangle & \langle \psi_{\tau_1}, \psi_{A_1} \rangle & \cdots & \langle \psi_{\tau_1}, \psi_{A_p} \rangle & \langle \psi_{\tau_1}, \psi_{\tau_1} \rangle & \cdots & \langle \psi_{\tau_1}, \psi_{\tau_p} \rangle \\ \vdots & \vdots & \ddots & \vdots & \vdots & \ddots & \vdots \\ \langle \psi_{\tau_p}, \psi_{A_0} \rangle & \langle \psi_{\tau_p}, \psi_{A_1} \rangle & \cdots & \langle \psi_{\tau_p}, \psi_{A_p} \rangle & \langle \psi_{\tau_p}, \psi_{\tau_1} \rangle & \cdots & \langle \psi_{\tau_p}, \psi_{\tau_p} \rangle \end{array} \right),$$

and similarly for  $\langle \Psi_\theta, \Psi_\theta^T \rangle_n$ . Using a similar notation, we compute the gradient vector as follows.

$$\begin{aligned} \frac{1}{n} \nabla_\theta &= \frac{1}{\sigma^2} \langle \Psi_\theta, \epsilon_\theta \rangle_n \\ &= \frac{1}{\sigma^2} (\langle \psi_{A_0}, \epsilon_\theta \rangle_n, \langle \psi_{A_1}, \epsilon_\theta \rangle_n, \cdots, \langle \psi_{A_p}, \epsilon_\theta \rangle_n, \langle \psi_{\tau_1}, \epsilon_\theta \rangle_n, \cdots, \langle \psi_{\tau_p}, \epsilon_\theta \rangle_n)^T, \end{aligned}$$

where  $\epsilon_\theta(t) = z(t) - y_\theta(t)$ .

Just as with i.i.d. observations, the MLEs are both consistent and asymptotically efficient under the assumption of normal errors.

**Theorem 4.1** *The maximum likelihood estimates are consistent; indeed, as  $n \rightarrow \infty$ , we have*

$$\sqrt{n} [(\tilde{\theta}, \tilde{\sigma}^2)^T - (\theta, \sigma^2)^T] \xrightarrow{d} N(0, I_{(\theta, \sigma^2)}^{-1}).$$

In order to compute the maximum likelihood estimate, we can use Fisher scoring as follows, taking the trigonometric moment estimates as the starting value.

$$\begin{pmatrix} \theta_{new} \\ \sigma_{new}^2 \end{pmatrix} = \begin{pmatrix} \theta_{old} \\ \sigma_{old}^2 \end{pmatrix} + \frac{1}{n} I_{(\theta, \sigma^2)}^{-1} \nabla_{(\theta, \sigma^2)} |_{(\theta_{old}, \sigma_{old}^2)}.$$

Because of the orthogonality of  $\theta$  and  $\sigma^2$ , we can first use Fisher scoring method to improve the estimate of  $\theta$ . This leads to the well known Gauss-Newton algorithm.

**Algorithm 4.1 Gauss-Newton.**

1. Let  $\theta_{old}$  be a  $\sqrt{n}$ -consistent estimate of  $\theta$ .
2. Calculate  $\theta_{new}$  by the following

$$\begin{aligned} \theta_{new} - \theta_{old} &= \frac{1}{n} I_\theta^{-1} \nabla_\theta |_{\theta_{old}} = [\langle \Psi_{\theta_{old}}, \Psi_{\theta_{old}}^T \rangle_n]^{-1} \langle \Psi_{\theta_{old}}, z - y_{\theta_{old}} \rangle_n \\ &= \left[ \sum_l \Psi_{\theta_{old}}(t_l) \Psi_{\theta_{old}}(t_l)^T \right]^{-1} \left[ \sum_l \Psi_{\theta_{old}}(t_l) (z(t_l) - y_{\theta_{old}}(t_l)) \right]. \end{aligned} \quad (13)$$

Although we can iterate the above procedure, the following result shows one step is enough for the consideration of efficiency.

**Theorem 4.2**

$$\sqrt{n}(\theta_{new} - \theta)^T \xrightarrow{d} N(0, I_\theta^{-1}).$$

Finally,  $\sigma^2$  can be estimated as

$$\sigma_{new}^2 = \left\| z(t) - A_{0,new} - \sum_{j=1}^p A_{j,new} w(t - \tau_{j,new}) \right\|_n^2.$$

## 5 Hypothetical regressions and model selection

In this section, we deal with the case of  $m$  unknown.

### 5.1 The least squares estimates and model fitting

Because of the linear dependence of the signal on the baseline and heights in a  $SC(w; p; \mathbf{A}; \boldsymbol{\tau})$ , once the number and locations of the peaks are obtained, we can use least squares to estimate the baseline and peak heights. Combining this idea with Algorithm 3.1, we are led to the following model fitting algorithm.

**Algorithm 5.1 Model-fitting.**

*Starting with the empirical trigonometric moments  $\hat{f}_k$ , for any given nonnegative integer  $m \leq K_0$ ,*

1. *Use the method of trigonometric moments to estimate the peak locations  $\{\bar{\tau}_j\}$  using Algorithm 3.1.*
2. *Eliminate those peaks falling outside  $[-\pi + \kappa_1, \pi - \kappa_2]$ , and denote the locations of the remaining peaks by  $\{\bar{\tau}_j, j = 1, \dots, \bar{m}\}$ , where  $\bar{m} \leq m$ .*
3. *Estimate the heights  $\bar{A}_j$  corresponding to these peaks by minimizing the following*

$$\left\| z(t) - \bar{A}_0 - \sum_{j=1}^{\bar{m}} \bar{A}_j w(t - \bar{\tau}_j) \right\|_n^2. \quad (14)$$

*This results in the least squares estimates of the baseline and heights.*

The output of this algorithm is a  $SC(w; \bar{m}; \bar{\mathbf{A}}^{(\bar{m})}; \bar{\boldsymbol{\tau}}^{(\bar{m})})$ . Next the problem of model selection arises because we can fit a spike-convolution model for each nonnegative integer in a given range.

### 5.2 Model selection

Suppose that the data is generated from a  $SC(w; p; \mathbf{A}; \boldsymbol{\tau})$ , and noise is added. In light of Theorem 2.1, models  $SC(w; \bar{m}; \bar{\mathbf{A}}^{(\bar{m})}; \bar{\boldsymbol{\tau}}^{(\bar{m})})$  with  $\bar{m} < p$  are not good. When  $\bar{m} \geq p$ , we might expect a subset of  $\{\bar{\tau}_j\}$  will be close to the real peak locations  $\{\tau_j\}$ . This is the basis of our model selection procedure, whose motivation will be clearer following the next result.

**Proposition 5.1** *Suppose that a Toeplitz matrix  $G_m$  has smallest eigenvalue  $A_0$  with multiplicity  $r > 1$ .*

1. Let  $m - r + 1 = p$ . Then the Toeplitz sub-matrix  $G_p$  has the same smallest eigenvalue  $A_0$  with multiplicity 1.
2. Let  $\{e^{i\tau_j}, j = 1, \dots, p\}$  be the roots corresponding to the eigenvector of  $G_p$  associated with the eigenvalue  $A_0$ . Then any polynomial whose coefficients form an eigenvector in the invariant space of  $G_m$  corresponding to  $A_0$  has  $\{e^{i\tau_j}, j = 1, \dots, p\}$  as a subset of its roots.

Let us consider Algorithm 3.1 in light of this result. Supposing that  $m \geq p$ , we explain the situation from two perspectives. From the computational perspective, in the absence of errors, any polynomial (not unique) whose coefficients form an eigenvector in the invariant space of  $G_m$  corresponding to the smallest eigenvalue always has  $\{e^{i\tau_j}, j = 1, \dots, p\}$  as a subset of its roots, where  $\tau_j$  are the real peak locations. But in general it is not true that all its zeros are on the unit circle. In the presence of errors, Theorem 3.2 implies that the multiplicity of the smallest eigenvalue is one (apart from a set of Lebesgue measure zero), and the resulting (unique) polynomial has all its roots on the unit circle. This attractive feature, in the computational sense, is the “positive” aspect of noise. From the perspective of spectral structures, the situation here has a close connection to the perturbation theory of matrices, see [8]. In the absence of errors, the distance between the invariant space  $\mathcal{S}$  of  $G_m$  corresponding to the smallest eigenvalue and other invariant spaces is positive. In other words, it is well separated from other invariant spaces. In the presence of errors and when the sample size is large enough, on the one hand, the last  $m - p + 1$  eigenvalues could be close to each other, and their eigenvectors could be “wobbly” (see [8]) under small perturbation of the noise. On the other hand the invariant space  $\hat{\mathcal{S}}$  defined by these possibly “wobbly” eigenvectors is stable. This is true because when the sample size is large enough,  $\hat{\mathcal{S}}$  is close to  $\mathcal{S}$ , which is well separated from other invariant spaces. Therefore we expect a subset of the roots obtained from Algorithm 3.1 to be close to  $\{e^{i\tau_j}, j = 1, \dots, p\}$  when the sample size is large enough. It is so because the eigenvector from which these roots are obtained belongs to  $\hat{\mathcal{S}}$ , and is close to one eigenvector belonging to  $\mathcal{S}$  and having the property as shown in Proposition 5.1. Now let us return to model fitting. The above argument means the regressors  $1, w(t - \bar{\tau}_1), \dots, w(t - \bar{\tau}_m)$  will include a subset of “explanatory variables” close to the true regressors  $1, w(t - \tau_1), \dots, w(t - \tau_p)$ . For large enough  $n$  we can therefore expect model selection criteria to behave as they do in the context of variable selection in regression. Our model selection procedure has two stages. We assume the model order has an upper bound  $M (\leq K_0)$ .

**Algorithm 5.2 Two-stage model selection.**

1. *First stage.* Among all the  $SC(w; \bar{m}; \bar{\mathbf{A}}^{(\bar{m})}; \bar{\boldsymbol{\tau}}^{(\bar{m})})$  models fitted by Algorithm 5.1, choose the one that minimizes the following

$$MGIC_1(r) = \bar{\sigma}(r)^2 + \frac{c_1(n) \log n}{n} r, \tag{15}$$

where  $\bar{\sigma}(r)^2$  is the quantity in (14), and  $c_1(n) \geq 0$  is a penalty coefficient. Denote this model by  $SC(w; \bar{m}_0; \bar{\mathbf{A}}^{(\bar{m}_0)}; \bar{\boldsymbol{\tau}}^{(\bar{m}_0)})$ .

2. *Second stage.* We regard the model selected in the first stage as a hypothetical regression model, and use a backward deletion procedure to select the final model. That is, starting

from  $SC(w; \bar{m}_0; \bar{\mathbf{A}}^{(\bar{m}_0)}; \bar{\boldsymbol{\tau}}^{(\bar{m}_0)})$ , we delete the peak that is least significant in terms of sum of squares. Compare the two models according to the following statistic

$$MGIC_2(r) = \check{\sigma}(r)^2 + \frac{c_2(n) \log n}{n} r, \quad (16)$$

where  $\check{\sigma}^{(r)2}$  is the sum of squares fitted by a model with  $r$  peaks, and  $c_2(n) > 0$  is another penalty coefficient possibly depending on  $n$ . Choose the one that minimizes  $MGIC_2$ . If one peak can be deleted according to this criterion, then we iterate this procedure until we cannot delete any more peaks.

We make some remarks about this procedure. First, existing model selection procedures such as AIC and BIC cannot be applied here, for the parameter estimates are not maximum likelihood ones. Second, the penalty term  $c_1(n)$  is used in the first stage to compare all models obtained from Algorithm 5.1, and overfitting is not suppressed but encouraged to some extent. In fact, we would like to find the "best overfitting" model in this stage. The penalty term  $c_2(n)$  is used in the second stage to eliminate those false peaks in the model obtained in the first stage. This suggests that we impose another restriction  $c_1(n) < c_2(n)$ . Third, the purpose of this two-stage model selection procedure is not only estimating the model order, but also producing a parameter estimate with much smaller bias and variance than that of the trigonometric moment estimate if the order could be assumed to be known, see the numerical example in Section 6 for details. Fourth, the determination of the two penalty terms needs more investigation in both theory and implementation, though some experience has been gained for the dataset we have been working on. Use of the bootstrap or cross validation is possible. For example, in the analogous problem of estimating the number of hidden frequencies in Model (4), Ulrych and Sacchi [31] chose the number using Kullback divergence as the risk, and a bootstrap method to estimate the risk of each model. Fifth, when applying this methodology to DNA sequencing data, we can set a lower bound as well as an upper bound on the model order, since the numbers of the four kinds of DNA bases in a given range can be estimated. Our experience shows moderate overfitting is not an issue for DNA traces. Finally, in the sequel, we refer to the procedures in Algorithm 3.1, 5.1, 5.2 as PDPS (parametric deconvolution of positive spikes). If the error distribution is known to be normal, Algorithm 4.1 (Gauss-Newton) could be included in PDPS to improve the accuracy of the estimate.

## 6 Examples and discussion

### 6.1 A simulated example

Our simulation study is based the following model.

#### Example 6.1

$$\begin{aligned} z(t_l) = & 0.5 + w(t_l + 1.9) + 1.25w(t_l + 1.6) + 1.25w(t_l + 1.3) + w(t_l) + \\ & 1.25w(t_l - 0.5) + 1.1w(t_l - 1.0) + 1.25w(t_l - 2.5) + \epsilon(t_l), \end{aligned}$$

where the sample size  $n = 1024$ ,  $w(t)$  is a Gaussian function  $\frac{b}{\sqrt{2\pi}} \exp\{-\frac{b^2 t^2}{2}\}$  with the scale parameter  $b = 8$  being truncated at  $\pm 4$  SD. Errors are normally distributed with mean 0 and standard deviation 0.3. Figure 2 shows a simulated sample from this model. The signal contains seven peaks,

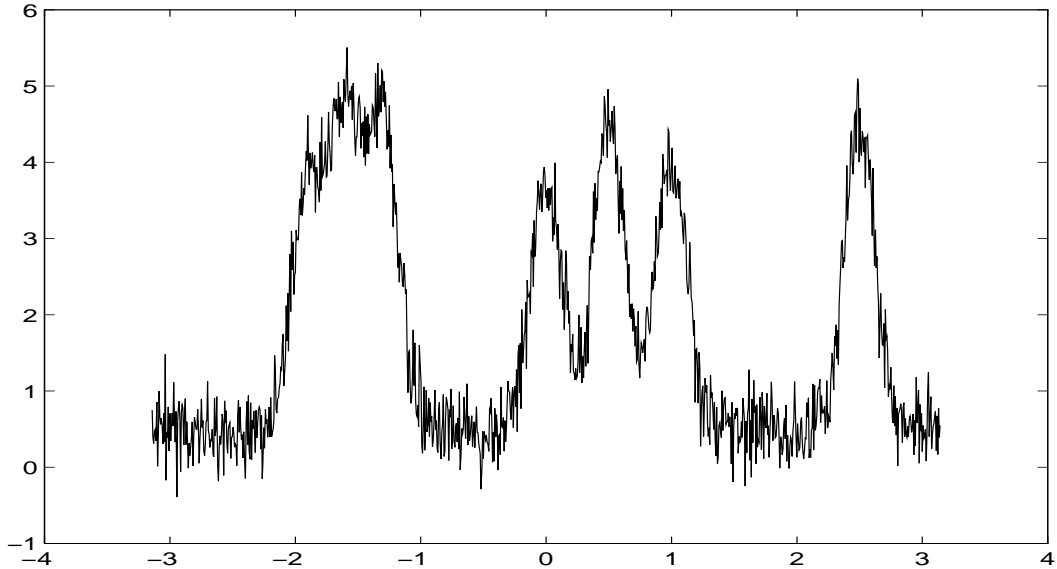


Figure 2: A simulated sample of Example 6.1

and the three on the left are quite close to one another. The peak heights are generally similar, which is typical for sequencing data. Simulations in this section are carried out in MATLAB, and are repeated 1000 times for each method we have studied. We apply three estimation procedures to this example. First, we assume the model order is known, and use the method of trigonometric moments. Second, we use PDPS to estimate the parameter. The penalty coefficients  $c_1(n)$  and  $c_2(n)$  are taken to be 2 and 10 respectively. The upper bound of the model order is taken to be 20. Out of the 1000 replications, all but one of the final-fitted models had order 7, which is the truth. Finally, this result was further tuned by the Gauss-Newton algorithm. Two iterations were used. The statistics of estimates of the peak locations and heights are summarized in Table 1. The estimate tuned by the Gauss-Newton algorithm is almost unbiased, and its standard errors are close to the nominal ones. It is quite surprising that the accuracy of the trigonometric moment estimate is so poor, even though the order is assumed to be known. In comparison, PDPS has achieved an accuracy much closer to that of the maximum likelihood estimate. This means that modest overfitting in the first stage can greatly control the bias and variance of the estimate. In other words, even when the number of peaks is known, PDPS is better than the direct trigonometric moment estimate in terms of bias and variance. In this case, we set a lower bound by the known order at the first stage, and stop the backward deletion when the number of left peaks equals the known order at the second stage. The frequency of the model orders selected at stage one is shown in Table 2. We see that most models selected at stage one have orders ranging from 9 to 12.

## 6.2 Real trace data

Next we apply PDPS to the sequencing trace shown in Figure 1. The point spread function is taken to be a truncated Gaussian function. The result is shown in Figure 3. (Maximum likelihood estimation was not used.) For a comparison, a nonnegative least squares deconvolution was carried out, see Lawson and Hanson [19]. The results are displayed in Figure 4. The two methods yield

parameter		Method of trigonometric moments			PDPS without MLE tuning			Gauss-Newton algorithm			
truth		bias ( $\times 10^3$ )	SD ( $\times 10^2$ )	CV (%)	bias ( $\times 10^3$ )	SD ( $\times 10^2$ )	CV (%)	bias ( $\times 10^3$ )	SD ( $\times 10^2$ )	CV (%)	Nominal SE ( $\times 10^2$ )
$\tau_1$	-1.9	-211	32		-8	2		0	0.4		0.4
$\tau_2$	-1.6	0	19		3	4		0	0.4		0.4
$\tau_3$	-1.3	315	48		11	2		0	0.3		0.3
$\tau_4$	0.0	64	14		-2	1		0	0.3		0.3
$\tau_5$	0.5	78	16		-2	1		0	0.2		0.2
$\tau_6$	1.0	97	26		-1	1		0	0.3		0.3
$\tau_7$	2.5	2	4		-6	1		0	0.2		0.2
$A_1$	1.0	-216	67	85	-8	11	11	0	2.1	2	2.1
$A_2$	1.25	506	20	11	52	6	5	0	2.1	2	2.1
$A_3$	1.25	-158	68	62	-30	11	9	-1	2.1	2	2.1
$A_4$	1.0	62	18	17	-1	2	2	0	1.7	2	1.7
$A_5$	1.25	21	8	6	-1	2	2	-1	1.7	1	1.7
$A_6$	1.1	-170	36	38	0	2	2	0	1.7	2	1.7
$A_7$	1.25	-9	13	10	-1	2	1	-1	1.7	1	1.7
$A_0$	0.5	-6	2	4	-1	2	3	1	1.3	3	1.2

Table 1: Statistics of the three estimates of the parameters in Example 6.1 (1000 replications).

model orders	8	9	10	11	12	13	14
frequency	48	248	212	202	244	45	1

Table 2: Frequency of model orders selected at the first stage.

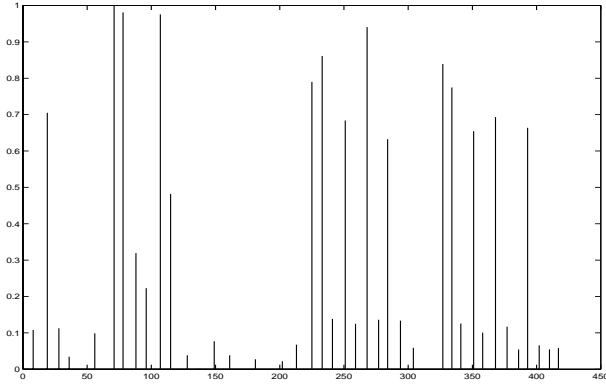


Figure 3: Parametric deconvolution.

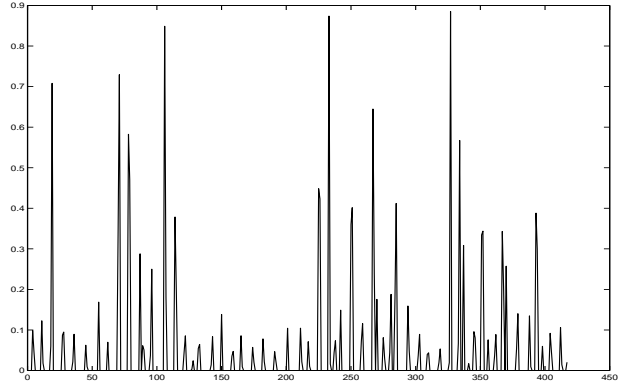


Figure 4: NNLS deconvolution (carried out by the Lawson and Hanson algorithm).

quite different results. First, that obtained from the parametric deconvolution is cleaner. Second, the relative heights of the major spikes following the parametric deconvolution are more similar to those in the original data. Third, parametric deconvolution is more efficient from the computational point of view. On a Sun Ultra-2 workstation, the Lawson and Hanson algorithm took more than one hour while the parametric method took only two minutes. A more systematic comparison of this parametric deconvolution method with others can be found in [20].

### 6.3 Colored noise and reblurring

The result in this paper can be generalized to situations when the errors are serially correlated. We might approximate such errors by an autoregressive process. That is, we could assume that the errors  $\epsilon$  in (2) can be modeled by

$$\epsilon_t + \sum_{k=1}^p \phi_k \epsilon_{t-k} = \xi_t, \quad (17)$$

where the  $\xi_t$  is i.i.d.  $N(0, \sigma^2)$ . Then we could prewhiten the signal as follows,

$$(\phi * z)(t) = (\phi * w * x)(t) + \xi(t). \quad (18)$$

By replacing  $z(t)$  by  $(\phi * z)(t)$ , we could use our original scheme PDPS to do the deconvolution. This reblurring idea have been used in other similar situations, see [7, 13].

### 6.4 Implementations

The numerical implementation of PDPS hinges on linear regression and computation of smallest eigenvalues and their eigenvectors of Toeplitz matrices. Because of the special structure of Toeplitz matrices, efficient algorithms do exist, and we refer to [12, 22]. Though we have discussed maximum likelihood estimates within the assumption of Gaussian errors in this paper, we may skip the MLE tuning in applications, since either the assumption of normal errors may not be appropriate, or highly accurate estimates of the peak positions and heights may not be necessary.

## 7 Appendix

This section contains the proofs and relevant mathematical facts. The following theorem is in essence the so called trigonometric moment problem solved by Carathéodory, see [9]. We present a version under the framework of the spike-convolution model.

**Theorem 7.1** 1. Given a  $SC(\delta; m; \mathbf{A}; \boldsymbol{\tau})$ , let  $G_m$  be the Toeplitz matrix constructed from its Fourier coefficients  $\{g_k\}$ . Then  $A_0$  is the smallest eigenvalue of  $G_m$  with multiplicity one and eigenvector  $(\alpha_0, \dots, \alpha_m)^T$ . The  $\{A_j\}$  satisfy the following linear system:

$$\frac{1}{2\pi} \begin{pmatrix} 1 & 1 & \cdots & 1 \\ e^{i\tau_1} & e^{i\tau_2} & \cdots & e^{i\tau_m} \\ \vdots & \vdots & \ddots & \vdots \\ e^{i(m-1)\tau_1} & e^{i(m-1)\tau_2} & \cdots & e^{i(m-1)\tau_m} \end{pmatrix} \begin{pmatrix} A_1 \\ A_2 \\ \vdots \\ A_m \end{pmatrix} = \begin{pmatrix} g_0 - A_0 \\ g_1 \\ \vdots \\ g_{m-1} \end{pmatrix}. \quad (19)$$

2. Conversely, suppose we are given  $2m+1$  complex numbers  $\{g_j, -m \leq j \leq m\}$ , where  $\overline{g_j} = g_{-j}$ . Assume that the smallest eigenvalue  $A_0$  of the Toeplitz matrix  $G_m = (g_{j-i})_{i,j=0,\dots,m}$  has multiplicity 1. Let the smallest eigenvector be  $\alpha = (\alpha_0, \dots, \alpha_m)^T$ , and  $U^{(m)}(z) = \sum_{j=0}^m \alpha_j z^j$ . Then there exists a unique  $SC(\delta; m; \mathbf{A}; \boldsymbol{\tau})$  whose first  $m+1$  Fourier coefficients are  $\{g_j, 0 \leq j \leq m\}$ . The  $\{\tau_j\}$  are determined from the  $m$  distinct roots  $\{e^{i\tau_j}\}$  of  $U^{(m)}(z)$  lying exactly on the unit circle. The  $\{A_j\}$  are determined by the linear system (19), and the resulting heights are positive.

**Proof:** The first part is easy to check. As for the second part, an algebraic proof can be found in [9]. Li [20] gives a measure-theoretic proof.

**Proof of Theorem 2.1:** Let the Fourier coefficients of the corresponding  $x(t)$  and  $\bar{x}(t)$  be  $\{g_k\}$ ,  $\{\bar{g}_k\}$  respectively. According to the Parseval identity,  $\|y - \bar{y}\|^2 = \sum_{k=-\infty}^{\infty} |v_k(g_k - \bar{g}_k)|^2 \geq (\min_{0 \leq k \leq p} |v_k|^2) \sum_{k=0}^p |g_k - \bar{g}_k|^2$ . Thus if there were a sequence  $SC(w; l; \hat{\mathbf{A}}^{(l)}; \hat{\boldsymbol{\tau}}^{(l)})$ ,  $l < p$  which could approach  $SC(w; p; \mathbf{A}; \boldsymbol{\tau})$ , then their Fourier coefficients  $\hat{g}_k^{(l)} \rightarrow g_k$ , for  $0 \leq k \leq p$ . Therefore their Toeplitz matrices  $\hat{T}_p^{(l)}$  will converge to  $T_p$  as do their characteristic polynomials. But this is impossible because  $T_p$ 's smallest eigenvalue has multiplicity 1 according to Theorem 7.1, while  $\hat{T}_p^{(l)}$ 's smallest eigenvalue has multiplicity larger than 1, as can be easily checked.

**Proof of Theorem 3.1:** This can be checked by direct calculation.

**Proof of Theorem 3.2:** By Theorem 7.1, we can find a function  $x$  of the form (1) with Fourier coefficients  $\{g_k\}$ . Next the proof is completed by convolving  $x$  with  $w$  and using the convolution theorem.

**Proof of Theorem 3.3:** Without loss of generality, assume  $n$  is even. A trigonometric moment  $\hat{f}_k$  can be decomposed into three parts,

$$\hat{f}_k = f_k + \sum_{l=-[\frac{n}{2}]}^{[\frac{n}{2}]-1} \left[ \frac{2\pi}{n} y(t_l) e^{ik t_l} - \int_{t_l}^{t_{l+1}} y(t) e^{ikt} dt \right] + \frac{1}{n} \sum_{l=-[\frac{n}{2}]}^{[\frac{n}{2}]-1} \epsilon(t_l) e^{ik t_l}, \quad (20)$$

for  $k = 0, \pm 1, \dots$ . Denote the second and third terms by  $\check{f}_k$  and  $\tilde{f}_k$  respectively. Suppose initially the order  $p$  of the model is known in advance, and let  $\hat{g}_0 = \check{f}_0$ ,  $\hat{g}_k = \check{f}_k v_0 / v_k$ , for  $0 < k \leq K_0$ .



Similarly, decompose  $\hat{g}_k$  into three parts,  $g_k$ ,  $\check{g}_k$  and  $\tilde{g}_k$  corresponding to  $f_k$ ,  $\check{f}_k$  and  $\tilde{f}_k$ , respectively. Under the smoothness condition on  $w(t)$ , the effect of  $\check{f}_k$  is of order  $O(1/n)$  using Taylor expansion and the bounded property of  $w'(\cdot)$ , and is thus negligible compared with that of  $\tilde{f}_k$ . Next, notice that  $\tilde{f}_k = \langle \epsilon(t), e^{ikt} \rangle_n$ . According to the Lyapunov Central Limit theorem,  $\tilde{f}_0, \tilde{f}_1, \dots, \tilde{f}_p$  are asymptotically normally distributed:

$$\sqrt{n}(\tilde{f}_0, \tilde{f}_1, \dots, \tilde{f}_p)^T \xrightarrow{d} N(0, \sigma^2 I_{p+1}).$$

Consequently, we have a CLT for the  $\hat{f}_k$ ,

$$\sqrt{n}[(\hat{f}_0, \hat{f}_1, \dots, \hat{f}_p)^T - (f_0, f_1, \dots, f_p)^T] \xrightarrow{d} N(0, \sigma^2 I_{p+1}).$$

Thus

$$\sqrt{n}[(\hat{g}_0, \hat{g}_1, \dots, \hat{g}_p)^T - (g_0, g_1, \dots, g_p)^T] \xrightarrow{d} N(0, \sigma^2 \text{diag}(|\frac{v_0}{v_k}|^2)).$$

For  $k \neq 0$ , we can split each term  $g_k$  into its real part  $g_{k,r}$  and its imaginary part  $g_{k,i}$ . Then another form of the above CLT is given by

$$\sqrt{n}[(\hat{g}_0, \hat{g}_{1,r}, \dots, \hat{g}_{p,r}, \hat{g}_{1,i}, \dots, \hat{g}_{p,i})^T - (g_0, g_{1,r}, \dots, g_{p,r}, g_{1,i}, \dots, g_{p,i})^T] \xrightarrow{d} N(0, P),$$

where  $P$  is given by (8). The mapping between the trigonometric moments and the parameters is continuous. Thus we can find the CLT for the trigonometric moment estimates using the delta method. Now we calculate the Jacobian matrix. From

$$\begin{pmatrix} g_0 \\ g_1 \\ \vdots \\ g_p \end{pmatrix} = \frac{1}{2\pi} \begin{pmatrix} 1 & 1 & 1 & \dots & 1 \\ 0 & e^{i\tau_1} & e^{i\tau_2} & \dots & e^{i\tau_p} \\ \vdots & \vdots & \vdots & \ddots & \vdots \\ 0 & e^{ip\tau_1} & e^{ip\tau_2} & \dots & e^{ip\tau_p} \end{pmatrix} \begin{pmatrix} A_0 \\ A_1 \\ A_2 \\ \vdots \\ A_p \end{pmatrix},$$

we have

$$\frac{\partial(g_0, g_1, \dots, g_p)}{\partial(A_0, A_1, \dots, A_p, \tau_1, \dots, \tau_p)} = \frac{1}{2\pi} \left( \begin{array}{c|ccc|ccc} 1 & 1 & 1 & \dots & 1 & 0 & 0 & \dots & 0 \\ 0 & e^{i\tau_1} & e^{i\tau_2} & \dots & e^{i\tau_p} & iA_1 e^{i\tau_1} & iA_2 e^{i\tau_2} & \dots & iA_p e^{i\tau_p} \\ \vdots & \vdots & \vdots & \ddots & \vdots & \vdots & \vdots & \ddots & \vdots \\ 0 & e^{ip\tau_1} & e^{ip\tau_2} & \dots & e^{ip\tau_p} & ipA_1 e^{ip\tau_1} & ipA_2 e^{ip\tau_2} & \dots & ipA_p e^{ip\tau_p} \end{array} \right).$$

Rewriting this as a square matrix by splitting the derivative into real and imaginary parts, we get

$$\frac{\partial(g_0, g_{1,r}, \dots, g_{p,r}, g_{1,i}, \dots, g_{p,i})}{\partial(A_0, A_1, \dots, A_p, \tau_1, \dots, \tau_p)} = \frac{1}{2\pi} Q.$$

Therefore  $V = 4\pi^2 Q^{-1} P (Q^{-1})^T$ . We refer to [24] for the invertibility of  $Q$ .

**Proof of Proposition 4.1:** This can be checked by direct calculation.

**Proof of Theorem 4.1**

1. Let  $l(\theta, \sigma^2)$  be the log likelihood evaluated at  $(\theta, \sigma^2)$ . To prove the consistency, we need to show that for any fixed  $(\theta_0, \sigma_0^2) \neq (\theta, \sigma^2)$ , where  $(\theta, \sigma^2)$  is the truth,

$$P(l(\theta_0, \sigma_0^2) < l(\theta, \sigma^2)) \longrightarrow 1, \quad \text{as } n \longrightarrow \infty \quad (21)$$

. Notice that

$$l(\theta, \sigma^2) - l(\theta_0, \sigma_0^2) = [l(\theta, \sigma^2) - l(\theta, \sigma_0^2)] + [l(\theta, \sigma_0^2) - l(\theta_0, \sigma_0^2)]. \quad (22)$$

Denote  $\theta_0 = (A_{0,0}, A_{1,0}, \dots, A_{p,0}, \tau_{1,0}, \dots, \tau_{p,0})^T$ , and let  $\eta(t) = y(t) - [A_{0,0} + \sum_{k=1}^p A_{k,0} w(t - \tau_{k,0})]$ . Then  $\int_{-\pi}^{\pi} \eta(t)^2 dt > 0$  for  $\theta_0 \neq \theta$  because of the identifiability of the parameterization.

By the law of large numbers, (cf. [2, 6]), the second term in (22) is,

$$\begin{aligned} \frac{1}{n}[l(\theta, \sigma_0^2) - l(\theta_0, \sigma_0^2)] &= \frac{1}{2n\sigma_0^2} \left[ \sum_l (\epsilon(t_l) - \eta(t_l))^2 - \sum_l \epsilon(t_l)^2 \right] \\ &= \frac{1}{2n\sigma_0^2} \left[ \sum_l \eta(t_l)^2 - 2 \sum_l \eta(t_l) \epsilon(t_l) \right] \xrightarrow{p} \frac{1}{2\sigma_0^2} \int_{-\pi}^{\pi} \eta(t)^2 dt \geq 0. \end{aligned}$$

The first term is:

$$\begin{aligned} \frac{1}{n}[l(\theta, \sigma^2) - l(\theta, \sigma_0^2)] &= \left[ -\frac{1}{2} \log \sigma^2 - \frac{1}{2n\sigma^2} \sum_l \epsilon(t_l)^2 \right] - \left[ -\frac{1}{2} \log \sigma_0^2 - \frac{1}{2n\sigma_0^2} \sum_l \epsilon(t_l)^2 \right] \\ &\xrightarrow{p} \left[ -\frac{1}{2} \log \sigma^2 - \frac{\sigma^2}{2\sigma^2} \right] - \left[ -\frac{1}{2} \log \sigma_0^2 - \frac{\sigma^2}{2\sigma_0^2} \right] \geq 0, \end{aligned}$$

since the function  $x(s) = -\log s - \frac{\sigma^2}{s}$  has its unique maximum at  $\sigma^2$ . Hence (21) is true.

2. Let  $D$  be the matrix with entries of second derivatives of the log-likelihood. Since the MLE  $(\tilde{\theta}, \tilde{\sigma}^2)$  is consistent, the following Taylor expansion can be checked straightforwardly,

$$\frac{1}{\sqrt{n}}[\nabla(\tilde{\theta}, \tilde{\sigma}^2) - \nabla(\theta, \sigma^2)] = \frac{1}{\sqrt{n}} D(\theta, \sigma^2) (\tilde{\theta} - \theta, \tilde{\sigma}^2 - \sigma^2)^T + O_p(\|(\tilde{\theta} - \theta, \tilde{\sigma}^2 - \sigma^2)\|^2). \quad (23)$$

Thus

$$\sqrt{n}(\tilde{\theta} - \theta, \tilde{\sigma}^2 - \sigma^2)^T \xrightarrow{d} - \left[ \frac{D(\theta, \sigma^2)}{n} \right]^{-1} \frac{\nabla(\theta, \sigma^2)}{\sqrt{n}},$$

where the first term converges to  $I_{(\theta, \sigma^2)}^{-1}$  in probability and the second term converges to  $N(0, I_{(\theta, \sigma^2)})$  in distribution. The remainder is an application of the Slutsky theorem.

**Proof of Theorem 4.2:** Notice that by Taylor expansion,

$$y_{\theta_{old}} - y = \Psi_{\theta}^T(\theta_{old} - \theta) + o_p(\|\theta_{old} - \theta\|),$$

where the second term is uniform with respect to the variable  $t$ , and so

$$z - y_{\theta_{old}} = \epsilon - (y_{\theta_{old}} - y) = \epsilon - \Psi_{\theta}^T(\theta_{old} - \theta) + o_p(\|\theta_{old} - \theta\|).$$

Inserting this into line 2 of the following, we obtain

$$\begin{aligned}
& \sqrt{n}(\theta_{new} - \theta) = \sqrt{n}(\theta_{new} - \theta_{old}) + \sqrt{n}(\theta_{old} - \theta) \\
= & \sqrt{n}[\langle \Psi_{\theta_{old}}, \Psi_{\theta_{old}}^T \rangle_n]^{-1} \langle \Psi_{\theta_{old}}, z - y_{\theta_{old}} \rangle_n + \sqrt{n}(\theta_{old} - \theta) \\
= & \sqrt{n}[\langle \Psi_{\theta_{old}}, \Psi_{\theta_{old}}^T \rangle_n]^{-1} \langle \Psi_{\theta_{old}}, \epsilon \rangle_n \\
& - [\langle \Psi_{\theta_{old}}, \Psi_{\theta_{old}}^T \rangle_n]^{-1} \langle \Psi_{\theta_{old}}, \Psi_{\theta} \rangle_n \sqrt{n}(\theta_{old} - \theta) \\
& + \sqrt{n}(\theta_{old} - \theta) + o_p(\|\sqrt{n}(\theta_{old} - \theta)\|) \\
\stackrel{p}{\rightarrow} & \sqrt{n}[\langle \Psi_{\theta}, \Psi_{\theta}^T \rangle_n]^{-1} \langle \Psi_{\theta}, \epsilon \rangle_n + \sqrt{n}[\langle \Psi_{\theta}, \Psi_{\theta}^T \rangle_n]^{-1} \langle \Psi_{\theta_{old}} - \Psi_{\theta}, \epsilon \rangle_n + o_p(1).
\end{aligned}$$

Here we need the  $\sqrt{n}$ -consistency of  $\theta_{old}$ . The second term in the last line is  $o_p(1)$ , since we can apply a Taylor expansion to  $\Psi_{\theta_{old}} - \Psi_{\theta}$  at  $\theta$ . Then we complete the proof by applying the central limit theorem to the first term and using the Slutsky theorem.

**Proof of Proposition 5.1:** The dimension of the invariant space corresponding to the smallest eigenvalue  $A_0$  is  $r$ . By Gaussian elimination, we can always find a vector in this space with the form  $\alpha = (\alpha_0, \dots, \alpha_p, 0, \dots, 0)^T$ . Of course,  $(\alpha_0, \dots, \alpha_p)^T$  is an eigenvector of  $G_p$  with eigenvalue  $A_0$ .  $A_0$  is the smallest eigenvalue of  $G_p$  because of the monotone property of eigenvalues of nested matrices. Its multiplicity is one. Otherwise, by repeating the above reasoning, we can find an eigenvector of  $G_{m-r}$  with the form of  $(\beta_0, \dots, \beta_{m-r})^T$ . Then by extending this vector into  $m+1$  Euclidean space by adding zeros in the beginning and the end, we can construct  $r+1$  linear independent eigenvectors of  $G_m$  corresponding to  $A_0$ , which would imply that the multiplicity of  $A_0$  is greater than  $r$ , a contradiction. In order to prove the second part, notice that  $(\alpha_0, \dots, \alpha_p, 0, \dots, 0)^T$ ,  $(0, \alpha_0, \dots, \alpha_p, 0, \dots, 0)^T$ ,  $\dots$ ,  $(0, \dots, 0, \alpha_0, \dots, \alpha_p)^T$  is a basis of the invariant space corresponding to  $A_0$ . Consequently, any polynomial whose coefficients are an eigenvector corresponding to  $A_0$  is a linear combination of polynomials with common roots  $\{e^{i\tau_j}, j = 1, \dots, p\}$ . The rest is obvious.

#### Acknowledgment

We give our grateful thanks to Prof. J. Rice for his very helpful comments. We owe many debts to the two referees. Their constructive suggestions have greatly enhanced this research and improved the organization of the material.

## References

- [1] M. D. Adams, C. Fields, and J. C. Ventor, editors. *Automated DNA sequencing and analysis*. Academic Press: London, San Diego, 1994.
- [2] P. Billingsley. *Probability and Measure*. John Wiley & Sons, 1986.
- [3] W.-Q. Chen and T. Hunkapiller. Sequence accuracy of larger DNA sequencing projects. *J. DNA Sequencing and Mapping*, 2:335–342, 1992.
- [4] V. Di Gesù and M. C. MacCarone. The Bayesian direct deconvolution method: properties and applications. *Signal Processing*, 6:201–211, 1984.
- [5] D. L. Donoho, I. M. Johnstone, J. C. Hoch, and A. S. Stern. Maximum entropy and the nearly black object. *Journal of the Royal Statistical Society, B*, 54(1):41–81, 1992.

- [6] R. Durrett. *Probability: Theory and Examples*. Wadsworth & Brooks/Cole, 1991.
- [7] D. R. Fredkin and J. A. Rice. *Fast evaluation of the likelihood of an HMM: ion channel currents with filtering and colored noise*. Department of Statistics, University of California, Berkeley, 1997.
- [8] G. H. Golub and C. F. Van Loan. *Matrix Computations*. The John Hopkins University Press: Baltimore and London, 3rd edition edition, 1996.
- [9] U. Grenander and G. Szegö. *Toeplitz Forms and Their Applications*. Berkeley and Los Angeles, University of California Press, 1958.
- [10] S. F. Gull. Developments in maximum entropy data analysis. In J. Skilling, editor, *Maximum entropy and Bayesian Methods*. Kluwer, Boston, 1989.
- [11] S. F. Gull and G. J. Daniell. Image reconstruction from incomplete and noisy data. *Nature*, 272:686–690, 1978.
- [12] D. Huang. Symmetric solutions and eigenvalue problems of Toeplitz systems. *IEEE Trans. Acoust., Speech. Signal Processing*, 40:3069–3074, 1992.
- [13] P. A. Jansson, editor. *Deconvolution of Images and Spectra*. Academic Press, New York, 1997.
- [14] T. J. Kennett, W. V. Prestwich, and A. Robertson. Bayesian deconvolution 1: convergence properties. *Nuclear Instrument and Methods*, 151:285–292, 1978.
- [15] T. J. Kennett, W. V. Prestwich, and A. Robertson. Bayesian deconvolution 2: Noise properties. *Nuclear Instrument and Methods*, 151:293–301, 1978.
- [16] T. J. Kennett, W. V. Prestwich, and A. Robertson. Bayesian deconvolution 3: application and algorithm implementation. *Nuclear Instrument and Methods*, 153:125–135, 1978.
- [17] B. F. Koop, L. Rowen, W.-Q. Chen, P. Deshpande, H. Lee, and L. Hood. Sequence length and error analysis of sequence and automated *taq* cycle sequencing methods. *BioTechniques*, 14(3):442–447, 1993.
- [18] C. B. Lawrence and V. V. Solovyev. Assignment of position-specific error probability to primary DNA sequence data. *Nucleic Acid Research*, 22(7):1272–1280, 1994.
- [19] C. L. Lawson and R. J. Hanson. *Solving Least Squares Problems*. Prentice-Hall, 1974.
- [20] L. Li. *Statistical Models of DNA Base-calling*. PhD thesis, University of California, Berkeley, 1998.
- [21] L. Li and T. P. Speed. An estimate of the color separation matrix in four-dye fluorescence-based DNA sequencing. *Electrophoresis*, 20:1433–1442, 1999.
- [22] J. Makhoul. On the eigenvectors of symmetric Toeplitz matrices. *IEEE Trans. Acoust., Speech. Signal Processing*, 29(4):868–872, 1981.

- [23] D. O. Nelson. Introduction of reptation. Technical report, Lawrence Livermore National Laboratory, 1995.
- [24] V. F. Pisarenko. The retrieval of harmonics from a covariance function. *Geophys. J. R. Astr. Soc.*, 33:347–366, 1973.
- [25] D. S. Poskitt, K. Dogancay, and S-H Chung. Double-blind deconvolution: the analysis of post-synaptic currents in nerve cells. *Journal of Royal Statistical Society, B*, 61:191–212, 1999.
- [26] W. H. Richardson. Bayesian-based iterative method of image restoration. *J. Opt. Soc. Am.*, 62(1):55–59, 1972.
- [27] L. A. Shepp and Y. Vardi. Maximum-likelihood reconstruction for emission tomography. *IEEE Transaction on Medical Imaging*, MI-1:113–121, 1982.
- [28] D. L. Snyder, T. J. Schulz, and J. A. O’Sullivan. Deblurring subject to nonnegativity constraints. *IEEE Transactions on signal processing*, 40(5):1143–1150, 1992.
- [29] P. B. Stark and R. L. Parker. Bounded-variable least-squares: an algorithm and applications. *Computational Statistics*, 10:129–141, 1995.
- [30] A. Tikhonov. Solution of incorrectly formulated problems and the regularization method. *Soviet Math. Dokl.*, 5:1035–1038, 1963.
- [31] T. J. Ulrych and M. D. Sacchi. Sompi, Pisarenko and the extended information criterion. *Geophysical Journal International*, 122:719–724, 1995.
- [32] Y. Vardi and D. Lee. From image deblurring to optimal investment: maximum likelihood solutions for positive linear inverse problems. *J. R. Statist. Soc. B*, 55(3):569–612, 1993.